Evidence of reverse and intermediate size segregations in dry granular flows down a rough incline

Nathalie Thomas, Umberto D 'Ortona

Evidence of reverse and intermediate size segregations in dry granular flows down a rough incline

Nathalie Thomas
*CNRS, Aix-Marseille Univ., IUSTI UMR 7343, 13453, Marseille, France**

Umberto D'Ortona
CNRS, Aix-Marseille Univ., Centrale Marseille, M2P2 UMR 7340, 13451, Marseille, France
(Dated: December 16, 2016)

In a dry granular flow, the position of a large tracer is numerically studied, first in a half filled rotating tumbler, then in a flow down a rough incline; all particles having the same density. Two (2D) and three (3D) dimensional cases are distinguished, with similar behaviours, but also discrepancies. In the tumbler, the tracer segregated position shows a progressive sinking towards the centre when increasing the size ratio between tracer and small beads, with a quantitative agreement with 3D experimental results. The tracer trajectory is studied to understand how it rapidly reaches and keeps an intermediate constant level during the flowing phase. For 3D thin flows down a rough incline, surface, intermediate and then reverse positions are successively obtained, with a continuous variation of the tracer depth. For 3D thicker flows on incline, the transition between surface and reverse segregations shows a strong discontinuity occuring on a short range of size ratios. Furthermore, for this sizes range, intermediate positions are confined in two thin zones, one just below the surface (but for which the tracer is not visible in surface) and one just above the bottom reverse segregation zone: intermediate segregation does not exist in the centre of the flow. The case of higher fractions of tracers on incline flows shows the three patterns, but with a less sharp transition, longer distances of convergence, and with a spreading of the tracers positions during the non stationary phase. The transition between surface and reverse segregation patterns is found around a size ratio 4.3 with a good agreement with experimental data.

PACS numbers: 45.50.-j 45.70.-n 45.70.Mg 45.70.Ht

I. INTRODUCTION

Size segregation in granular flow is a phenomenon that has been extensively studied [1–9]. Nevertheless, only in year 2000, reverse and intermediate segregations of particles of different sizes and same density were first observed experimentally in granular flows [10]. When a few large tracers are flowing with small particles (size ratio of tracer size on small beads size higher than 4), the large particles do not reach the surface like in classical surface-segregation, but rather stabilise either at an intermediate level (intermediate segregation) or at the bottom of the flow (reverse segregation). This progressive sinking of large beads when increasing their size ratio has been interpreted as a mass effect, being enhanced (resp. reduced) by an increase (resp. a decrease) of the density of the large particle [11]. Let us note that reverse segregation was also obtained in vibrated granular systems [12–14]. The origin of this 'reverse Brazil nuts effect' is due to high amplitude vibrations inducing an inertia driven segregation process [12, 15] or to the absence of convective motion [16].

We define the 'reverse segregation' in a rotating half filled cylindrical tumbler when large particles are close to the tumbler centre (taking into account the thickness of the flowing layer) in the solid rotating part. At the opposite, the large particles having a small size ratio (from 1.5 to 3) end up at the periphery, undergoing a 'surface-segregation'. For a flow down an incline, a fraction of 10% of large 'reverse-segregated' particles disappear from the surface while flowing, and are present near the bottom of the deposit. The same phenomenon was observed in the case of a flow feeding a heap: very large particles forming a core in the heap of small particles, instead of a ring of large particles at the periphery of the heap, as in the case of small size ratios [10].

We define the 'intermediate segregation' in the tumbler, when large particles are found at an intermediate radius in the solid rotating part (Fig. 1), that corresponds for most of the cases to an intermediate level in the flowing layer. This happens for size ratios ranging from 4 to approximately 15, for small fractions of large particles (3%) [10]. All radii have been precisely measured and decrease continuously with the increasing size ratio, corresponding to the height in the flow passing continuously from the surface to the bottom. The limit between reverse and intermediate cases is not precise. A radial reverse position should correspond to a tracer touching the bottom of the flowing layer, but this point of view is complicated by the fact that the bottom of the flow will be defined (here) by an averaging of small beads streamlines. Note that the tracer has almost no effect on this averaging process. Yet, the tracer can deform the loose material below and around it. We will compare radial positions and positions within the flow of the tumbler whenever it is possible.

* nathalie.thomas@univ-amu.fr

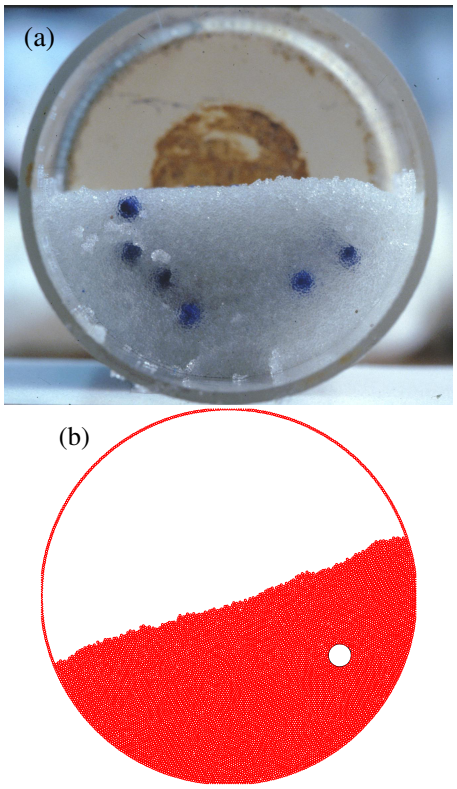

FIG. 1. A $D = 4.85$ cm rotating cylindrical tumbler with $d = 0.3$ mm small beads and $d_t = 3$ mm large beads (tracers). *(a):* One slice of an experiment done with 3% blue tracers, slowly impregnated with water after the flow has stopped and before to be sliced [10]. *(b):* 2D simulation with one tracer.

For a flow down a solid rough incline, the intermediate segregation is defined when large particles are found at intermediate levels inside the deposit. However, our experiments in the case of the flow down an incline were not precise enough to assess the existence of an intermediate segregation on an incline [10]. Even if the mean location of the large beads in the deposit varies continuously with the size ratio from the top to the bottom, there was a large spatial spreading of the positions for these intermediate levels. Furthermore, this could be related to a non-stationary state of the flow, and/or to the aggradation during the stopping phase of the flow that could modify the position of the tracers. For that reason, we focus this paper on a numerical study of the reverse and intermediate segregations during flows on incline to gain a better understanding of the phenomena, without any stopping phase.

The existence or non existence of intermediate equilibrium positions for a tracer in a granular flow down an incline is the main question of this article. Therefore, the migration of a unique large tracer in a flow of small particles is first extensively studied for several size ratios, assuming that several identical tracers would flow at the same depth and cluster in a segregation pattern. The case of several tracers, 5% to 10%, is also considered and compared with the case of one tracer. It allows a confrontation with previous experiments [10] made with 10% of tracers.

This article is organised as follows: in the second section, the numerical method is presented. In section 3, the method is validated in a rotating cylindrical tumbler in two (2D) and three dimensions (3D) through a comparison with 3D experimental results of segregation. In section 4, the displacement of tracers in a granular flow down an incline is studied in 2D, and in 3D. Then, a study of multiple tracers flow on incline and a confrontation with experiments in channel is presented. The article ends by conclusions.

II. THE NUMERICAL METHOD

The numerical method used is distinct element method (DEM). A linear-spring and viscous damper force model [17, 18] was used to calculate the normal force between contacting particles: $\mathbf{F}_{ij}^n = [k_n\,\delta - 2\gamma_n m_{\text{eff}}(\mathbf{V}_{ij}\cdot\hat{\mathbf{r}}_{ij})]\hat{\mathbf{r}}_{ij}$ where δ and $\mathbf{V}_{ij} = \mathbf{V}_i - \mathbf{V}_j$ are the particle overlap and the relative velocity of contacting particles respectively, $\hat{\mathbf{r}}_{ij}$ is the unit vector in the direction between particles i and j, $m_{\text{eff}} = m_i m_j/(m_i + m_j)$ is the reduced mass of the two particles, $k_n = m_{\text{eff}}[(\frac{\pi}{\Delta t})^2 + \gamma_n^2]$ is the normal stiffness and $\gamma_n = \ln e\,/\Delta t$ is the normal damping with Δt the collision time and e the restitution coefficient.

A standard tangential force with elasticity was implemented: $\mathbf{F}_{ij}^t = -\min(|\mu\mathbf{F}_{ij}^n|, |k_s\zeta|)\text{sign}(\mathbf{V}_{ij}^s)$ where $\mathbf{V}_{ij}^s$ is the relative tangential velocity of the two particles, k_s is the tangential stiffness, and $\zeta(t) = \int_{t_0}^{t}\mathbf{V}_{ij}^s(t')\,\mathrm{d}t'$ is the net tangential displacement after contact is first established at time $t = t_0$. The gravitational acceleration was $g = 9.81\,\mathrm{m\,s^{-2}}$. The particles properties correspond to cellulose acetate: density $\rho = 1308\,\mathrm{kg\,m^{-3}}$, restitution coefficient $e = 0.87$ and friction coefficient $\mu = 0.7$ [17, 19–21]. To avoid a close-packed structure, the particles had a uniform size distribution ranging from $0.95d$ to $1.05d$. The collision time was $\Delta t = 10^{-4}$ s, consistent with previous simulations [21–23] and sufficient for modeling hard spheres [24–26]. These parameters correspond to a stiffness coefficient $k_n = 7.32\times10^4$ N m^{-1} [17] and a damping coefficient $\gamma_n = 0.206$ kg s^{-1}. The integration time step was $\Delta t/50 = 2\times10^{-6}$ s to meet the requirement of numerical stability [24].

Rough incline and tumbler walls were modeled as a monolayer of bonded particles of the same size. Tumbler wall is composed of small particles that rotate in a solid way. In the simulations of incline, small beads are placed randomly in the simulation domain and as gravity was set, they fall on a sticky plane. All small beads touching the bottom of the domain ($z = 0$) do not move anymore and form the rough plane of the incline. The other ones constitute the flowing granular material. With that procedure, rough inclines with compacity around 0.57 were obtained in 3D. A large tracer is placed, usually at the top of the free surface, and at time zero, gravity is tilted from

0 to $\theta = 20°$ in 2D or to 23° in 3D (except where stated), and the flow starts. For tumblers, the large tracer is placed first, randomly inside the drum, or at a defined location, if needed. The other flowing particles are then placed randomly inside the tumbler. At time zero, the gravity is switched on, flowing particles fall and wall particles start their rotation movement. In tumblers and inclines, wall particles had an infinite mass for calculation of the collision force between flowing and fixed particles. The velocity-Verlet algorithm was used to update the position, orientation, and linear and angular momentum of each particle. Periodic boundary conditions are applied in the directions x or x-y of the box (flow direction or flow - horizontal directions) in the case of an incline, and along the tumbler horizontal axis y in the case of a 3D cylinder. In the tumbler case, velocity maps are obtained by binning particles. From these maps, streamlines and velocity profiles are extracted. Velocity maps have been obtained either including the tracer, or excluding the tracer in the binning, or by generating a monodisperse flow where the tracer was replaced by exactly the same volume of small particles. All obtained velocity maps are identical.

III. ROTATING CYLINDRICAL TUMBLERS

The aim of this part is to obtain results in 2D, and 3D rotating cylindrical tumblers, to compare them precisely with 3D experimental results. This will provide a validation for the numerical method and some insights on the process happening during the flow.

The experiments have used glass beads of different diameters and of the same density. In the experimental rotating cylindrical tumbler (4.2 cm long and 4.85 cm in diameter), only a few (typically 50) large beads, named tracers, were initially placed such that they nearly do not interact. The diameter of the tracers ($d_t = 3$ mm) was kept constant while the size of the small particles decreased from $d = 2.5$ mm to $d = 90$ μm to explore size ratios ranging from $d_t/d = 1.2$ to 33. The cylinder was half filled with a mixture of large and small beads and was rotated at about 3.6 rpm in order a continuous flow develops with a flat free surface. After three revolutions, a stationary state was reached, and tracers had nearly reached identical radial positions leading to a half-ring segregation pattern (Fig. 1(a)). Since each radius in the solid rotating part corresponds to a level during the flow, we interpreted a segregated ring by the fact that all its tracers had the same preferential height within the flow. The radial segregated position R_t is defined as the mean of all tracers radial positions R_{ti}.

From a numerical point of view, this experimental protocol is not easy to reproduce since the number of small particles increases strongly, reaching 10^5 for the case of 90 μm small particles in 2D, and even more in 3D. First, we will use a model as close as possible to the experimental protocol, but in 2D. In a second time, we will change the tracer size (with care) to reach larger size ratios.

A. 2D simulations of rotating tumbler

1. *Direct comparison with experiments*

The 2D numerical tumbler of inner diameter $D = 2R = 4.85$ cm is half filled with monodisperse small beads and one large tracer of the same density. Small beads vary from 2.5 mm to 90 μm in diameter and the large tracer is 3 mm. The tumbler turns around its axis at a speed of 15 rpm to ensure a continuous flow with a flat free '1D surface'.

Figure 2 shows one trajectory of a large tracer ($d_t/d = 16$) passing successively through the flowing layer and the solid rotating zone. After a few revolutions (4 to 5, not shown here), the trajectory converges and fluctuates around an equilibrium radial position: a stationary state is reached. Each time i the tracer passes through the vertical plane $x = 0$ in the static rotating zone, the distance of the centre of the tracer from the centre of the cylinder R_{ti} is measured: a mean position R_t and a standard deviation are computed. Small standard deviations indicate a strong localisation at the same radius, that corresponds to a segregation since several non interacting tracers would segregate at this same position. R_t is called the segregation position, it corresponds to the experimental segregation half ring radius (for an experimental/simulation comparison see Fig. 1).

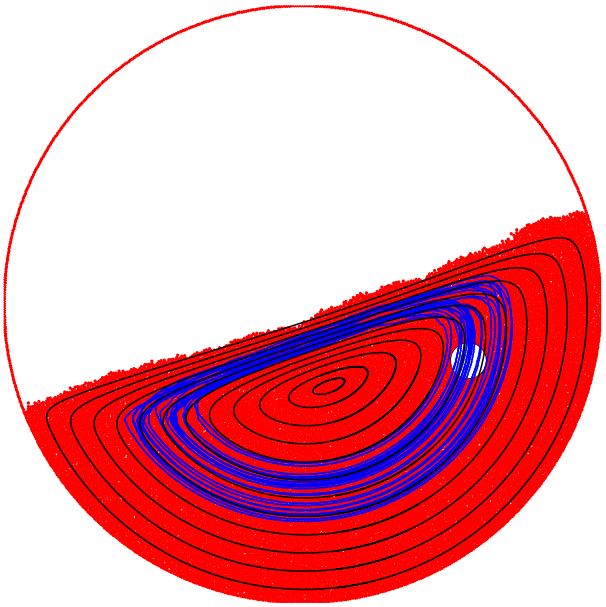

FIG. 2. A 4.85 cm diameter rotating tumbler with 187 μm small beads and a 3 mm white tracer, $d_t/d = 16$. The blue line is the trajectory of the tracer. The tracer segregates at intermediate level and radius. Black lines are streamlines of the red small beads.

As in the experiments, we observe surface-segregation of the smaller tracers (large tracers go at the periphery), then an intermediate segregation (large tracers remain at an intermediate radius as in Fig. 2), and a progres-

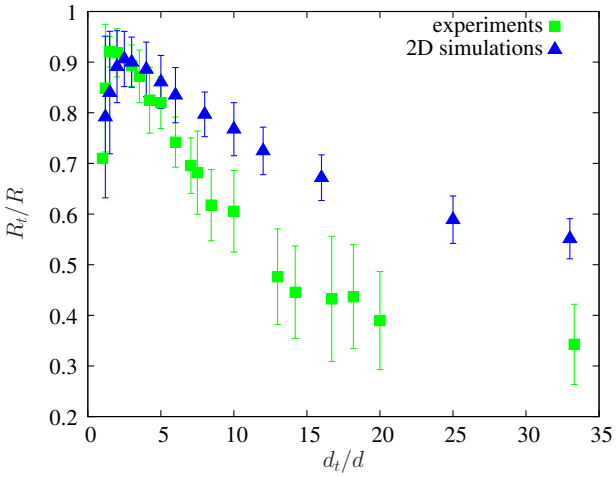

FIG. 3. Relative positions of the tracers in the cylindrical tumbler versus size ratio d_t/d for 3D experiments (green ■) ([11]) and 2D simulations (blue ▲). Errors bars represent standard deviations.

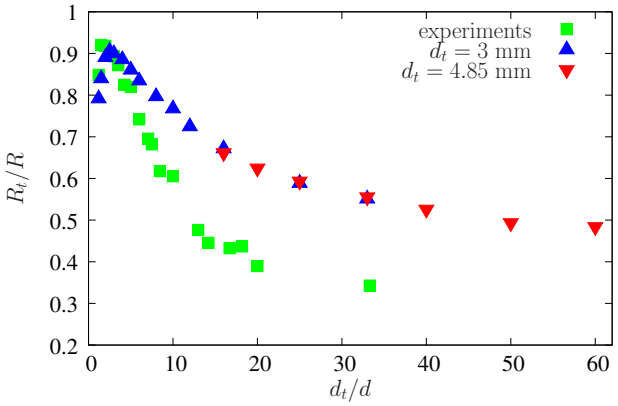

FIG. 4. Relative positions of the centre of tracers in the tumbler versus size ratio d_t/d, for 3D experiments ([11]) and 2D simulations, with D =4.85 cm and 2 tracer sizes, 3 and 4.85 mm.

sive sinking as their size ratio increases. The agreement between experiments and simulations is good with a similar evolution of the curve of the radial position versus the size ratio, but only qualitative (Fig. 3). Differences exist when comparing 3D experiments and 2D simulations. (1) In 3D experiments, the decrease of the curve R_t/R versus d_t/d is more rapid than in 2D simulations. (2) In 2D simulations, the asymptotic value of the curve is close to 0.55, a larger value than the asymptotic value of the 3D experimental case, around $R_t/R = 0.35$. This 2D asymptotic value will not be reduced for larger size ratios (Fig. 4). (3) Another difference is observed on the maximum of the curve (surface-segregation), which occurs for $d_t/d = 1.5$ or 1.8 in experiments, instead of $d_t/d = 2.5$ in the 2D simulations (Fig. 3). We will see that these differences are due to the 2D character of these simulations rather to an experiment-simulation discrepancy. A longer discussion on that point is made when 3D simulations data are presented.

2. *Higher size ratios*

To reach higher size ratios, the number of particles to simulate needs to be reduced. Several tracer sizes have been tested ($d_t = 3$, 4.85, 6 and 9.7 mm) in the tumbler $D = 48.5$ mm, and the equilibrium positions R_t reached by the tracers were compared. Up to a diameter of $d_t =$ 6 mm, equilibrium positions are almost identical. For the larger tracer ($d_t = 9.7$ mm, to be compared with the drum diameter $d_t = D/5$), a small discrepancy (relative error of 4%) was observed in the equilibrium position. We choose to keep the size of the tracer under $d_t = D/10$ to be sure that no effect comes from the tracer size.

A tracer diameter $d_t = 4.85$ mm is adopted to reach high size ratios up to 60. Figure 4 shows the relative positions of the 3 mm and 4.85 mm tracers, compared to 3D experimental results. When the 2 different tracers have the same size ratio d_t/d, the resulting positions well superimpose. For the largest size ratios of these 2D simulations, the radial position slowly decreases but remains close to 0.5, and does not reach the experimental value of 0.35. Asymptotic R_t values between 2D simulations and 3D experiments are different. Even if the qualitative behaviour is reproduced, 3D simulations are needed for a precise comparison.

B. 3D rotating tumblers

1. *Comparison with experiments*

To obtain a quantitative agreement, 3D simulations, as shown in Fig. 5, have been performed. The tumbler inner-diameter is equal to $D = 48.5$ mm and rotates around the y axis. In a first series (size ratio up to 8), the tracer diameter is set to $d_t = 3$ mm as in experiments, then for larger size ratios (from 5 to 25) to $d_t = 4.8$ mm, to reduce the number of small beads simulated. For size ratios $d_t/d = 5$ and 8, both tracers size have been tested. Larger tracers ($d_t = 6$ and 9 mm) have also been used to check the sensibility to the tracer size. Like in 2D, no differences were observed for a 6 mm tracer, and very small discrepancies for 9 mm.

The equilibrium radius of the tracer (Fig. 6) quantitatively agrees with the 3D experimental data. Agreement is very good even on precise points like the slope of the curve, the asymptotic value of R_t/R for high size ratios, or the diameter ratio which corresponds to the maximum of the radial position R_t/R. We are confident in our simulation method to study other systems, as flows on rough inclines.

Another question is how to interpret the different values of R_t/R in terms of segregation within the flowing

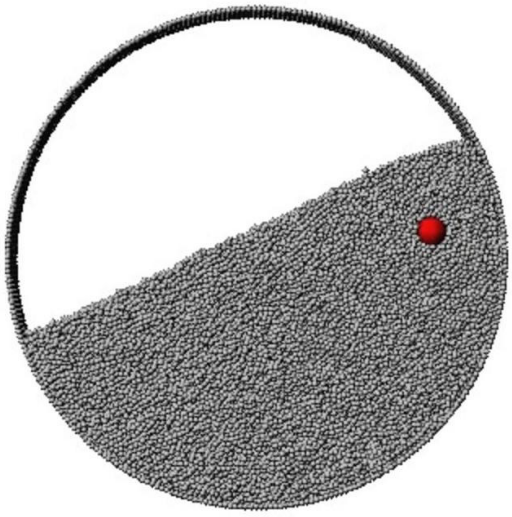

FIG. 5. Picture of a 3D simulation of a rotating cylinder (48.5 mm in diameter) with a 3 mm tracer immersed in 0.5 mm small beads.

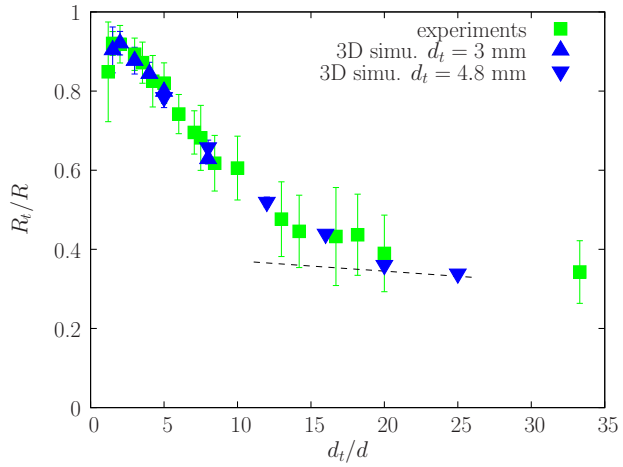

FIG. 6. Relative positions of the centre of the tracers in the tumbler versus size ratio d_t/d, in 3D experiments and 3D simulations. Dashed line is the position of a tracer touching the bottom of the flow.

layer of the tumbler, to anticipate a link between conclusions of the tumbler and the incline studies. In particular, is the asymptotic low value of R_t/R a possible reverse segregation? Note that a constant reverse position in the flow would undergo a little decrease of R_t/R, because with our protocol, the thickness of the layer (=minimum of R_t) slightly decreases. Our numerical thickness measurements (added with a tracer radius) draw the dashed line (on Fig. 6), i.e. the positions where a tracer touches the bottom. Size ratios 20 and 25 are in reverse segregation, and the small decrease between them is explained. In addition, in some simulations, we measure the depth of the tracer on its trajectory. For a ratio 8, (see below, Fig. 7(b)) the tracer is at an intermediate level. For the highest size ratios (for example 20): the tracer is just on the bottom of the flowing layer (i.e. the tracer bottom passes where streamlines are reduced to the stagnation point, which is nowhere else than the bottom layer centre). Even if it is difficult to defined the bottom of a flowing layer on a loose and deformable granular matter which could be modified by the tracer itself, we then choose to call 'reversed' the positions of these highest ratios. However, we keep in mind that it is arbitrary: the bottom of the flowing layer is defined by an averaging of small beads streamlines, and the tracer passage has almost no effect on the averaging, although it probably deforms locally and during a short time, the granular material around it, when it passes 'at the bottom'. With that choice, the rather central R_t/R positions (near 0.35) correspond to a tracer at a reverse bottom position within the flow.

2. Differences between 2D and 3D tumblers

The 2D study presents few differences with the 3D case, interpreted as a reduced effect of the size ratio, compared to the 3D case: the maximum of the curve happens later, the slope is less steep, and the asymptotic value is higher. First, we had to check that the difference 3D-2D is not due to a difference of thickness of the flowing layer, but they have been measured nearly identical, for a given size ratio, in 2D and 3D simulations. We compare for a size ratio (d_t/d =20) the level of the tracer within the flow. In 3D, the tracer is touching the bottom, while in 2D, the tracer is flowing above the bottom having 6 small beads below it. The delay in R_t/R positions does correspond to a delay in depth positions in the flowing layer.

For the highest tracers in 2D (above 40), we measure that the tracer touches the bottom of the flowing layer (bottom defined as explained above). Thus, they exhibit a reverse segregation within the flow, while being considered in a radial intermediate position. Asymptotic R_t/R values in 2D are greater than those in 3D, although they both correspond to tracers in reversed position in the flow, with our way to define the bottom. This remark shows how it is difficult to understand precisely what happens in the flow tumbler, when positions are close to the centre, i.e. close to the loose granular material below the flow. The way that particles pass from static to flow plays a role in the process, role which begins to be important when close to the centre. Obviously, the process is different in 2D and 3D, giving different asymptotic values.

Nevertheless, there is a real delay of the evolution of the 2D curve compared to 3D curve (also on the flow positions, not only on R_t/R), even far from the tumbler centre. To understand the cause of this delay, one should compare the effective densities of the media made of small particles. If we note ρ the density of the (large or small) beads, the effective density of the granular media made

of small beads is equal to $c\,\rho$ where c is the compacity. In other words, a large bead is denser than a sphere of the same diameter, but filled with a random close packing of small beads. In 2D, such a packing gives a compacity closed to $c_{2d} \simeq 0.8$, while in 3D, $c_{3d} \simeq 0.6$. Thus, the density ratio between the tracer and the media is larger in 3D than in 2D, leading to a deeper segregation. This result was confirmed using tracers of decreasing densities [11]. For tracers less dense than a random packing media of the small beads, only surface segregation of the tracer was observed.

Even if the names of the segregation patterns are arguable, there are similarities but also discrepancies between 2D and 3D cases. In 3D, the evolution of the position shows an advance of the curve maximum and a steeper dependence with the size ratio. Moreover, the link between level and radius behaves differently for the highest size ratios. The enhance of the effect of the size ratio is due to the compacity around 0.6 (in 3D) or 0.8 (in 2D) and we expect that it will always be present in all types of flow. Thus, 2D studies should be taken with care if extrapolated to the 3D case.

3. *Trajectories in tumbler*

Figure 7(a) shows the trajectory of a large particle with a size ratio 4 and the streamlines of small beads. Two phases are distinguished: first, the unsteady stage, second a stationary trajectory when segregation level is reached.

The tracer initially falls after tumbler have been filled (vertical line), then the rotation starts with the tracer relatively close to the stagnation point. During the first, second, third, and beginning of the fourth passage in the flowing layer, the tracer shows an up motion when compared to the small beads streamlines. It migrates towards its equilibrium position. Accordingly, in the static zone, from one passage to the following, the radial position R_{ti} increases. Then, after these 4 passages, the trajectory is stationary: the tracer flows parallel to streamlines at each pass, and presents a nearly constant radial position R_{ti} with some fluctuations from turn to turn. The segregation process happens mainly during the flow, and is not due to processes happening during the entrance and/or the exit from the flowing layer. Here, the tracer has started from a central position, and the motion is upward to reach its balance level. It could have been downward if the tracer would have started from the surface. An equivalent upward motion is observed for a tracer with a size ratio 8 (Fig. 7(b)), but with a smaller amplitude as the starting position is closer to the corresponding equilibrium R_t/R, than for the ratio 4 case.

Once in the steady phase, the tracer trajectory and small beads streamlines are parallel in the flowing zone. There is no relative up or down motion anymore. Plotting a circle of 3 mm on the trajectory, shows that the tracer of size ratio 4 is just below the surface, and that the tracer of size ratio 8 is on intermediate segregation. Each level in the flowing layer corresponds to one radius in the rotating part of the tumbler. However, the tracer trajectory does not match the same streamlines in the rotating zone and in the flowing zone. There are two small shifts between tracer trajectory and small beads streamlines when going in and out the flowing layer. At

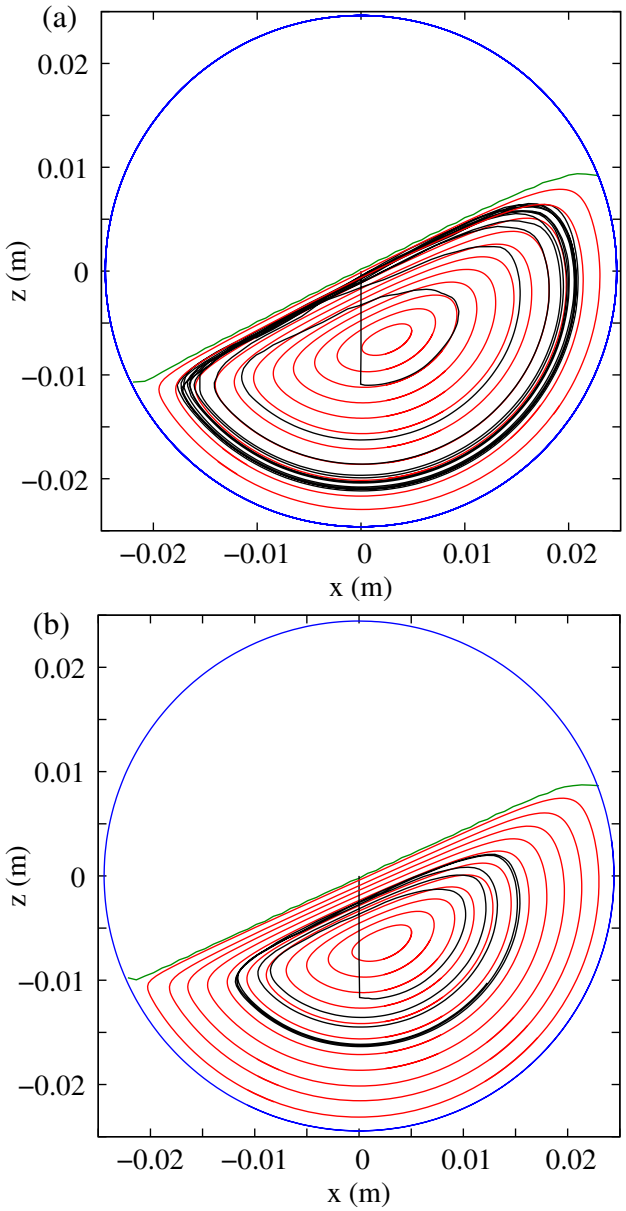

FIG. 7. Trajectory (black line) of the tracer centre, and streamlines (red lines) of small beads ($D = 48.5$ mm, $d_t = 3$ mm). The first rotations concern the convergence, when the tracer crosses streamlines. The followings, the stationary phase, where the tracer flows parallel to streamlines: (a) for $d_t/d = 4$, the tracer is just at the limit between surface and intermediate segregation, as its top is touching the free surface (green line), (b) for $d_t/d = 8$, the tracer is on an intermediate position.

the entrance (Fig. 7(b)), the tracer starts to move after the small beads of the same streamline (despite the shift of the previous exit), probably because its bottom is still surrounded with non moving small beads. At the exit of the flow, the tracer stops before the small beads of its corresponding streamline because its lower part is touching the static curved bottom. Note that this behaviour is the opposite of what happens when large beads segregates at the surface of a flow, where they flow further away than small beads, partially rolling on them. We conclude that these shifts are not responsible for the segregation, from turn to turn. But they exist, probably vary with R_t and might be the cause for the discrepancy between 2D and 3D asymptotic values. For that reason, it is not possible to easily deduce flowing height positions from both data of streamlines of small particles and R_t/R. Nevertheless, if not too close to the centre, these shifts are little. The R_t/R variation comes mainly from a level variation within the flowing layer.

When looking precisely, the entrance in the flow induces a starting point slightly above the balance level that the tracer will reach (Fig. 7(a)). At each pass in the flowing layer, tracer exhibits a tiny decrease towards its balance level, then keeps a constant level for the end of the flow, parallel to streamlines. The length at which the constant level is reached (approximately at mid length for ratio 4, almost immediately for ratio 8) seems to decrease with the tracer size (Fig. 7). Segregation is so fast, that a slight destabilisation can be rebalanced in each flow pass.

In conclusion, the trajectories study in the 3D cylindrical tumbler shows that the process responsible for the segregated radial positions of tracers is a vertical migration and stabilisation of the tracer at various depths, occuring during the flow. We then expect a similar phenomenon to happen during a flow on an incline. In addition, as 3D numerical modeling of tumblers shows a good quantitative agreement with experiments, we are confident to explore the case of the rough incline.

IV. ROUGH INCLINE

The experimental study of granular segregation occuring in a flow down an incline is a very difficult task to achieve in large channels (3D). Indeed, in our experimental study, only the surface of the flow was visible. The volume of the deposit could be accessed after the flow has stopped due to a slope change or a vertical end wall [10]. For large size ratios ($d_t/d \geqslant 6$), no tracers were visible at the surface during the flow. The large particles were found inside the deposit, more or less near the bottom. But it was not possible to conclude if tracers found at an intermediate height in the deposit were flowing at this level (corresponding to an intermediate segregation) or have ended there during the aggradation of the deposit.

The main advantage of the incline geometry is that height measurements of tracers in flows are direct, while measurements of radii in the cylinder, even if they are strongly linked to the height of the tracers during the flow, implies also entrance, acceleration and stop phases. Moreover, the solid rough bottom level of the incline is well defined, which is not the case in a partially filled tumbler where flows pass on loose granular matter, with a curved geometry. Another difference is that the flow thickness in the tumbler is mainly imposed by the geometry (tumbler and small particles sizes). For the chosen protocol (decreasing small bead size), this layer thickness decreases with the size ratio (around $8d$ for $d_t/d = 2$; $21d$ for $d_t/d = 10$; $34d$ for $d_t/d = 25$). While for confined flows on incline, the thickness of the flow can be varied independently. The smallest chosen thickness is comparable to those encountered in non confined flows on incline (around $10d$) [27], and, for this reason, the results on such thin flows do not lack of interest. The numerical thickness will then be increased to explore the effect of this parameter, and to reach the experimental value of the confined channel for comparison [10].

As experimental results were not obtained following any protocol, we choose to kept the small beads diameter constant (6 mm), and vary the size of the tracer, because to decrease the size of the small beads would have increased the velocity of the flow and the time of calculation, even for a constant flow thickness. Nevertheless, we may expect some deviations between experimental and numerical results if tracer size becomes too large compared to the flow thickness.

A. 2D simulations of flows on incline

1. *Intermediate segregation*

Even if quantitative agreement is not guaranted, 2D simulations are easy to conduct, allow a large variation of all possible parameters and have shown interesting results in the cylinder. Simulation boxes are $160d$ long, or $300d$ long for the larger tracers. Figure 8 shows a 48 mm diameter tracer in a granular flow made of 6 mm disks flowing down an incline. The incline slope is 20° and the thickness of the flow h_{max} is around 36 cm. The

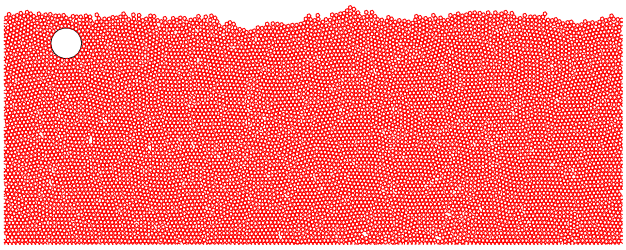

FIG. 8. Picture of a 2D granular flow down a rough incline with 6 mm small beads and a 48 mm large tracer, flowing from left to right. The angle of the slope is 20°, the thickness is 36 cm.

tracer with this size ratio ($d_t/d = 8$), is not far from the free 'surface', but remains below it, at an intermediate level. This does not correspond to the classical granular surface-segregation of large particles, but to a particle flowing inside, at a constant depth corresponding to an intermediate segregation.

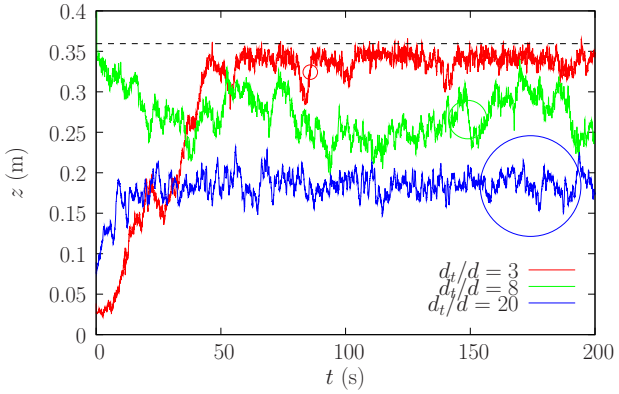

FIG. 9. Vertical position of the centre of 3 tracers versus time. The horizontal dashed line indicates the free 'surface'. Circles show the size of the three tracers, to be compared with the thickness of the flow.

Figure 9 shows the vertical position $z(t)$ of the centre of several tracers with three different sizes versus time t (each simulation has a single tracer). Several initial positions, at the bottom or surface, have been tried for each tracer size, but here, only one has been plotted. The final position h does not depend on the initial location. For the size ratio $d_t/d = 8$, corresponding to Fig. 8, the tracer almost never reaches the free surface and stays at an intermediate level. It is the most noisy trajectory. At intermediate levels, the trajectory is not stabilised by the existence of the free 'surface' or of the bottom nearby. For the size ratio $d_t/d = 20$, the tracer reaches an equilibrium position located near the centre of the flow. That keeps a layer of 22 small beads below the large tracer. The tracer $d_t/d = 3$, initially placed at the bottom of the flow, reaches the surface showing a surface segregation.

For the size ratio $d_t/d = 16$, both trajectories, released from the top or from the bottom, reach the same equilibrium position in about 10 s (Fig. 10). For the smaller size ratio ($d_t/d = 3$), the tracer starting at the bottom of the flow has to cross the all granular thickness, with a trajectory showing larger fluctuations to reach the surface and, then, needs a longer time (around 50 s) to reach its equilibrium position.

To study where the segregation would focus the tracers, the mean vertical position of one tracer is reported in the stationary regime for several size ratios d_t/d (keeping $d = 6$ mm) and for several thicknesses of the flow (Fig. 11). The mean location h sinks with increasing size ratios, as R_t/R does in the tumbler. Moderately large tracers ($2 \leqslant d_t/d \leqslant 6$) are found at the surface, with a maximum for a size ratio between 2 and 3. Positions seem related to the distance from the free surface, inde-

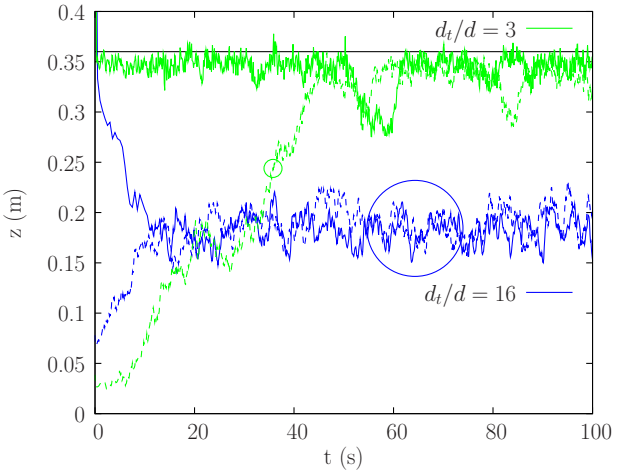

FIG. 10. Vertical position of 2 tracers $d_t/d = 16$, released at the top (solid lines) and the bottom (dashed lines) of the flow. Both trajectories converge to the same equilibrium vertical position. A tracer with $d_t/d = 3$, released at bottom undergoes surface segregation. Circles show the tracer sizes and the horizontal black line marks the mean position of the free 'surface'.

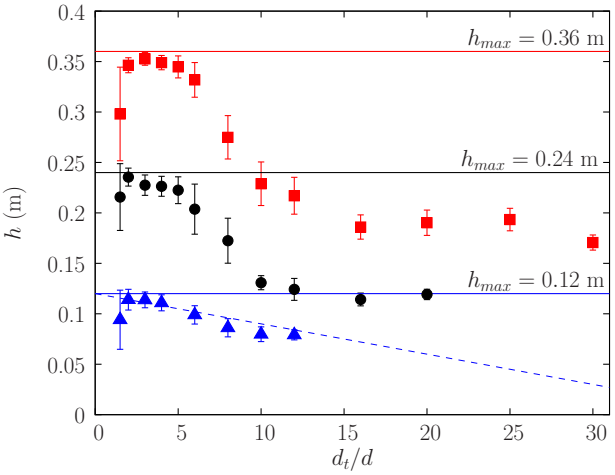

FIG. 11. Positions of the tracers in a flow down a 2D incline versus size ratio, for 3 flow thicknesses: (blue ▲) 0.12 m, (black ●) 0.24 m, (red ■) 0.36 m. Error bars show the standard deviations of the vertical position. Horizontal lines show the positions of the free 'surfaces'. Oblique dashed line corresponds to a tracer position whose summit would be at the surface of the thinnest flow.

pendently of the thickness of the flow. For larger size ratios ($d_t/d \geqslant 7$), the tracer sinks down the granular flow. The asymptotic value for high size ratios is close to $h_{max}/2$, which scales with the thickness of the flow. The interesting result is that tracers stabilise at different intermediate levels inside the flow, showing the existence of an intermediate segregation in a 2D flow on a rough incline. The small standard deviations, represented as error bars, mean that each large tracer does not explore the whole thickness of the flow, but remains at some in-

termediate well defined height, with little randomness in its trajectory. Note that for thin flows, size ratios above 10 are very large compared to the thickness of the flow, tracers are close to appear at the surface although they interact with the bottom at the same time. The oblique line shows the position of a tracer so its top is flush with the free surface of the flow. It provides a tool to define a surface/intermediate segregation limit (for low size ratios), but also shows the reasonable maximum size for a tracer in thin flows (here, a ratio 12).

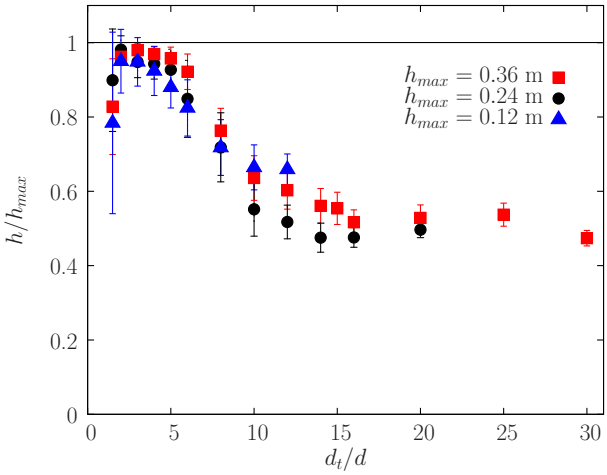

FIG. 12. Relative positions of the tracer centre in the flow down a 2D incline vs size ratio, for three flow thicknesses: (blue ▲) 0.12 m, (black ●) 0.24 m, (red ■) 0.36 m.

If the vertical position is renormalised by the thickness of the flow (Fig. 12), the three previous curves collapse reasonably well. Let us also note that in the classical surface-segregation pattern ($1.5 \leqslant d_t/d \leqslant 6$), a rescaling like $h_{max} - h$ is a better choice as curves match well in their upper part, but the curves will no more collapse for large size ratios. The segregation in a 2D flow shows two regimes: a first one (surface segregation) where the position depends on the distance to the surface, independently of h_{max} value, and a second one, where the position is intermediate, inside the flow and towards $h_{max}/2$, which scales with the flow thickness.

The positions h show that only surface and intermediate segregation patterns are obtained in 2D granular flows on incline. The large tracer does not reach positions below than half of the flow height, even for very high size ratios. For the thinnest flow, positions are compatible with a reverse segregation considering the low number of small beads below the tracer, but for thicker flows both types of segregation are possible to differentiate, and we see that segregated positions end up really at mid-flow for high ratios. The largest tracer have 14 small beads below it, in the thickest flow. Since, in tumblers, the position evolution vs size ratio is enhanced in 3D, compared to the 2D case, we expect different results on 3D incline. Another point worth noting is that the slope of the curve h (or R_t/R) vs d_t/d is steeper for a 2D incline than for a 2D tumbler and that the asymptotic value is approached for lower size ratios in incline.

2. *Slope angle*

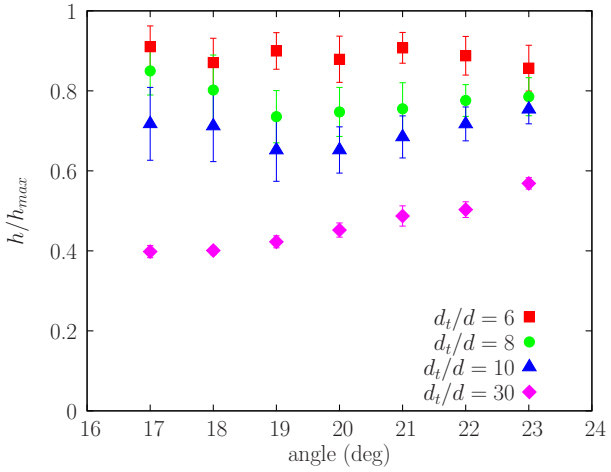

FIG. 13. Relative positions of the tracers in a 2D incline flow vs slope angle ($\theta = 17$ to $23°$) for 4 size ratios: $d_t/d = 6$, 8, 10 and 30. The thickness of the flow is $h_{max} = 36$ cm.

In a granular flow down an incline, the easiest way to increase the shear rate, without changing the thickness of the flow, is to increase the slope. Figure 13 plots the relative position of four tracers, with size ratios $d_t/d = 6$, 8, 10 and 30, for several tilt angles of the incline. Even if small evolutions are measurable, the relative vertical position is almost unchanged for a slope change from 17 to 23°, inducing an increase of the mean velocity of the flow, and thus of the shear rate, by a factor of 4.

B. 3D flows on incline

A series of simulations have been performed in the 3D case, first in a thin flow, then in thicker flows. Even if very high size ratios are not reachable with our computational facilities, it captures most of the phenomena and allows a comparison with the 2D case and with the experiments in 3D channel.

1. *Equilibrium positions*

Figure 14 shows a typical 3D flow, with a size ratio $d_t/d = 6$. As the tracer usually remains inside the flow, not visible, all the small beads on the right side of the tracer have been removed to draw the picture. The horizontal dimensions of the simulation domain are $20d \times 20d$ (0.12 m × 0.12 m) or ($40d \times 40d$) for the larger size ratios. Both domain sizes have been used for several size ratios to be sure that the simulated domain is large

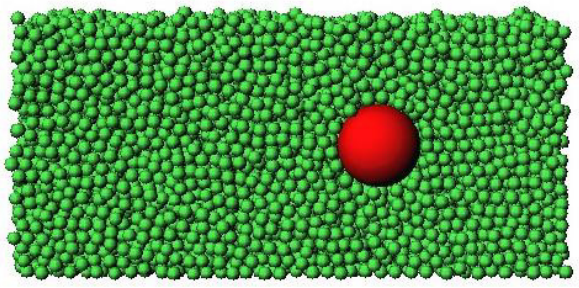

FIG. 14. Image of a 3D granular media with a tracer ($d_t/d = 6$) flowing from left to right down an incline (slope is 23°, $h_{max} = 0.112$), side beads have been removed to show the tracer.

enough. The thickness ($h_{max} = 0.112$ m $\simeq 18d$) corresponds to a relatively thin flow, comparable to the flows encountered in our 3D tumbler for size ratios around 8. The tilt angle is 23°.

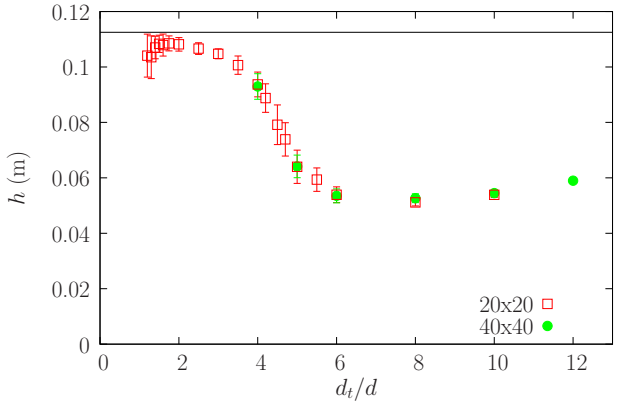

FIG. 15. Vertical positions of the tracer centre in the flow down a 3D incline versus size ratio d_t/d. The error bars represent the standard deviations, the horizontal line is the free surface ($h_{max} = 0.112$ m, slope is 23°). Two domain sizes have been used: $20d \times 20d$ (red □) and $40d \times 40d$ (green •).

Figure 15 plots the equilibrium vertical positions of the tracer (from 7.2 to 72 mm in size) for size ratios ranging from $d_t/d = 1.2$ to 12. For each size ratio, the large tracer position evolves rapidly during the flow (see below Figs. 16 and 17) to finally stabilise at a constant depth h. Some tracer have been initially placed at the bottom of the flow, and some at the surface with no final difference. Once on steady state, fluctuations are small and lead to small standard deviations in h positions. The final depth h depends on the size ratio between tracer and small beads (Fig. 15).

Like in the 3D rotating tumbler, the maximum of the curve (i.e. tracer at the free surface) is obtained for size ratios between 1.5 and 1.8 (Fig. 15). For size ratios between about 4 and 6, the tracer reaches an equilibrium height inside the flow, suggesting the existence of an intermediate segregation in 3D flow incline. For the larger size ratios, $d_t/d > 6$, the equilibrium positions reach a saturation value near the bottom. We note that the equilibrium positions are independent of the size of the simulation box. The slight increase of the curve for the higher size ratios (10 and 12) is due to the increase of the size of the tracer itself compared to the thickness of the flow, the tracer having only about 4 small beads below it.

Comparing 3D and 2D cases (Figs. 12 and 15), the overall behaviour is the same but a few differences are present. In the 3D case, the equilibrium position decreases more rapidly and reaches a low saturation value for size ratios close to $d_t/d = 6$, instead of $d_t/d = 10$ or 15 in 2D. We also note that the standard deviations are much smaller in 3D.

2. *Thickness of the flow*

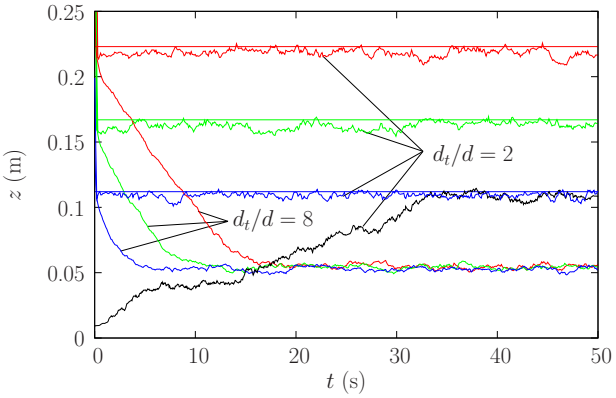

FIG. 16. Trajectory of the tracers in the flow down a 3D incline (slope is 23°) for 2 size ratios, $d_t/d = 2$ and 8, and 3 flow thicknesses, $h_{max} = 0.112$ m, 0.167 m and 0.223 m.

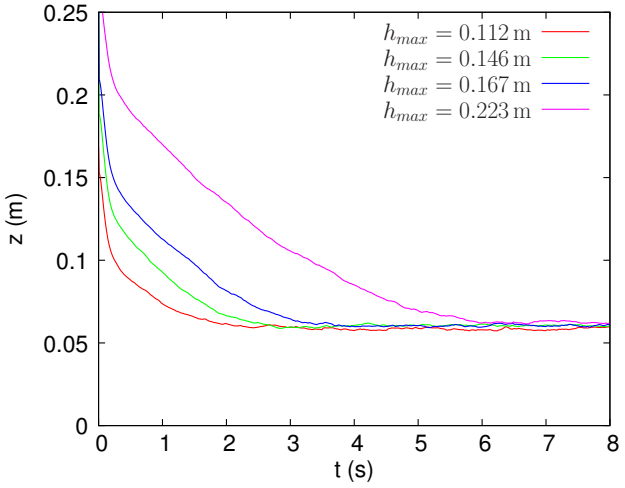

FIG. 17. Time evolution of a tracer centre height ($d_t/d = 12$) in a 3D incline for 4 flow thicknesses (slope is 23°). Tracer is initially placed on the surface.

Figure 16 shows the trajectories for the first 50 s of two tracers, $d_t/d = 2$ and 8, immersed in granular flows having three different thicknesses. The horizontal continuous lines show the free surfaces of the flows: $h_{max} = 0.112$ m, 0.167 m and 0.223 m. For the three thicknesses, the tracer with a size ratio of 2 remains, or goes at the surface of the flow showing a classical granular surface-segregation (only the thinnest flow have been shown for the ratio 2 tracer placed at the bottom). When crossing the whole thickness, the convergence is longer for a small size ratio ($d_t/d = 2$) than for a large one ($d_t/d = 8$), and the trajectory presents more fluctuations. The large tracer ($d_t/d = 8$) sinks near the bottom of the flow and reaches a stationary height close to 0.05 m, independently of the thickness of the flow. As the tracer radius is $r_t = 0.024$ m, it does not touch the rough incline made of small glued beads, but about 4 small beads remains between the tracer and the incline. Parallel trajectories (also on Fig. 17) show that, for a given size ratio, the time of convergence is mainly related to the thickness of material to travel through. But comparing different size ratios shows that convergence is more rapid for the size ratio 12 than 8 (Figs. 17 and 16), or 8 than 5 (see later Fig. 23(b)). Forces down acting on tracers are stronger when tracers are larger, and so heavier.

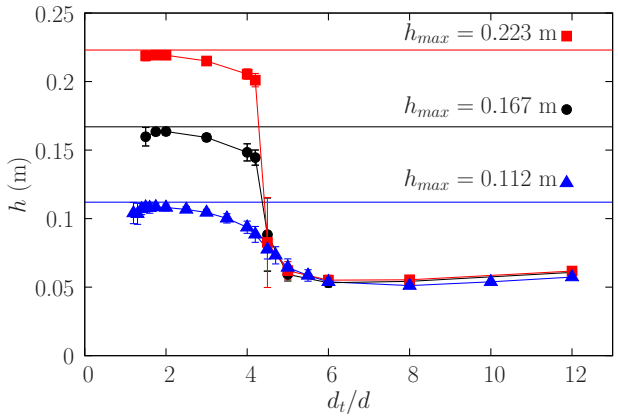

FIG. 18. Equilibrium vertical positions of the tracers versus size ratio, for 3 different thicknesses of the 3D flow, h_{max}: (blue ▲) 0.112 m, (black ●) 0.167 m, (red ■) 0.223 m. The error bars show the standard deviations of the vertical positions.

Figure 18 shows the equilibrium position h of a large tracer versus size ratio for three different thicknesses. For size ratios up to 4, the large tracer remains at (or close to) the surface, independently of the thickness h_{max}. For size ratios larger than 5, the tracer sinks close to the bottom of the flow, and (as in Fig. 16) h is independent of the thickness of the flow. For the two thicker flows, a sharp transition from the classical segregation to the inverse segregation appears for a size ratio d_t/d between 4.2 and 5. While a progressive variation is observed for the thinnest flow. The tracer position h depends on the thickness of the flow only during the transition. Both other h evolutions, for small or high size ratios, are independent of h_{max}.

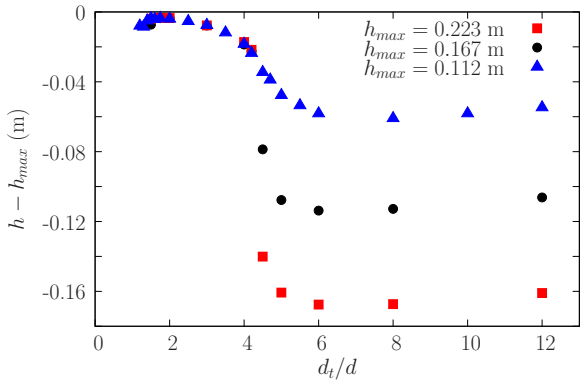

FIG. 19. Equilibrium vertical positions of the tracers compared to the surface position, for 3 different thicknesses of the 3D incline flow: (blue ▲) 0.112 m, (black ●) 0.167 m, (red ■) 0.223 m.

Plotting h (Fig. 18) shows that the distance to the bottom controls the position for very large tracers, independently of the thickness of the flow. In the same way, plotting $h - h_{max}$ (Fig. 19) shows that the distance at the surface is independent of the flow thickness for moderately large tracers ($1.5 < d_t/d < 4.5$), when classical surface-segregation occurs. It seems that two independent phenomena, one coming from the presence of the surface and one from the bottom, influence the segregated final position. In the case of a thin flow, the two phenomena interact by getting close, and the result is a more progressive transition between the two influences, creating a larger range of intermediate segregation positions. In the case of a thick flow both influences are separated, and could be studied independently.

It could be tempting to associate the three zones to the surface, intermediate and reverse segregations. But for example, tracers just below the surface (as for a ratio 4) are not visible in surface, and they should be considered in intermediate segregation. In a symmetric way, for example, the tracer with a ratio 5 is floating above the larger ones, and is in intermediate segregation, although the largest tracers (above 6) which show a slight increase of the centre position due to their size increase, are in strong interaction with the bottom incline and, then, are in reverse segregation. It seems that either the separation in the segregation into three patterns is not representative of the phenomena happening in the granular matter, either we have to split the surface flow zone in two layers (one corresponding to a surface segregation, and one to an intermediate segregation), and to split the bottom flow zone (one layer with intermediate segregation, one with reverse segregation) (Fig 20). In this last point of view, thin flows have two intermediate segregation layers (those touching the surface segregation layer and those

touching the bottom reverse segregation layer) continuously connected, forming a "large" central one. Although thick flows, have their two intermediate segregation layers separated by a empty central zone in the flow, where no tracer segregates.

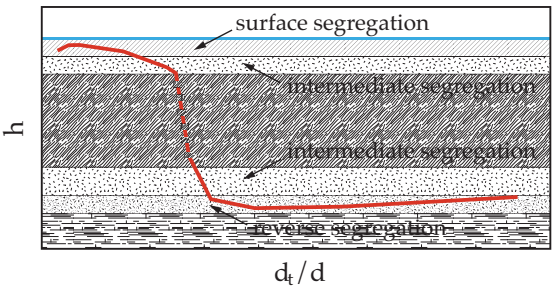

FIG. 20. The surface zone, split in two, surface and intermediate segregation layers, and the bottom zone, split in two, intermediate and reverse segregation layers. Red curve is from Fig. 18. In a thick flow, there is a layer in the centre with no segregation equilibrium positions in it. For a thin flows, both intermediate segregation layers merge, giving a 3 layers system. The bottom is never reached, part due to the size of the tracer itself and part due the presence of few (around 4) small beads below the tracer.

The fact that for $h_{max} = 0.112$, the asymptotic equilibrium height is close to $h_{max}/2$ (Fig. 15), as in the 2D case, is just a coincidence, since the asymptotic value in 3D is independent of h_{max}. The main difference between 2D and 3D is the equilibrium height of very large tracers (Figs. 11 and 18). The large tracers sink near the bottom, exhibiting a reverse segregation in the 3D case, while they locate in an intermediate segregation in 2D. The fact than the one process (in 2D) is h_{max} dependent, although the other one (in 3D) is independent of h_{max}, shows how the segregations of large tracers in 2D and 3D are different processes. Moreover, the transition between classical segregation and reverse segregation is steeper in 3D than in 2D cases (see Fig. 12). The transition occurs between size ratios $d_t/d = 4$ and 6, while in 2D, all the transition occurs between $d_t/d = 5$ and 15. This steeper evolution in the 3D case (compared to the 2D case) is also observed in the tumbler. Nevertheless, similar behaviours are also noticed for small size ratios in 2D and 3D: the tracers positions are both related to the distance to the surface, independently of the h_{max} value, nevertheless the maximum is not reached for the same size ratio in 2D and 3D. As for the tumbler system, the 2D incline case should not be extrapolated in 3D without care: evolutions with size ratio are different, which is due to the compacity difference in 2D or 3D, even if some similarities for small size ratios are observed.

3. *Comparison between tumbler and incline*

Flows on inclines propagate on solid rough surfaces while, in tumblers, flows pass on a loose curved granular material. As the evolutions of the curves of the 'vertical' position h (or R_t/R) in the flow vs d_t/d are similar in both type of flows (incline or tumbler), their comparison gives informations on the difference coming from the structure of the flow. Figure 21 shows the normalised positions in the flows on the incline h^* and the radial positions R_t/R in the tumbler at the same scale (we choose to adjust the minimal and maximal positions of h to the minimum and maximum values of R_t/R). The curves match relatively well for $d_t/d \leqslant 3.5$, indicating that for these small size ratios the process is mainly controlled by surface phenomena, which are quite insensitive to the substratum. For higher ratios $d_t/d \geqslant 4$, curves shift with a steeper slope for the case of the rough inclines. The difference comes from those of the substratum. In 2D, similar results are obtained. One more time, like in Figs. 18 and 19, data suggest that the segregation comes from the addition of one phenomenon due to the presence of the surface, and one due to the presence of the bottom.

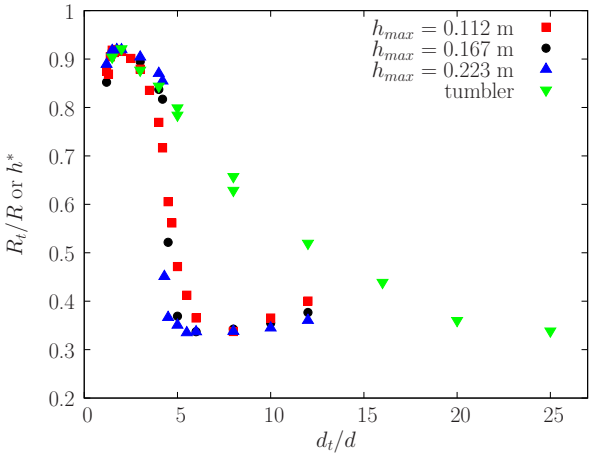

FIG. 21. Equilibrium positions of the tracer versus size ratio, for the 3D tumbler (green ▼) and equivalent rescaled positions for the 3D incline flows with 3 thicknesses, h_{max}: (red ■) 0.112 m, (black ●) 0.167 m, (blue ▲) 0.223 m.

4. *Slope angle*

Several simulations have been done for different slope angles. Low and high size ratios show no dependence with slope, i.e. with the velocity of the flow (Fig. 22(a)). On the contrary, when getting close to the size ratio that corresponds to the transition between surface and reverse segregation (between 4 and 6), the equilibrium position depends on the slope. The greater the angle, the deeper the large tracer is. We interpret that by the fact that the flow being more rapid, it looses cohesion and is no

more able to carry large and consequently heavy tracer anymore.

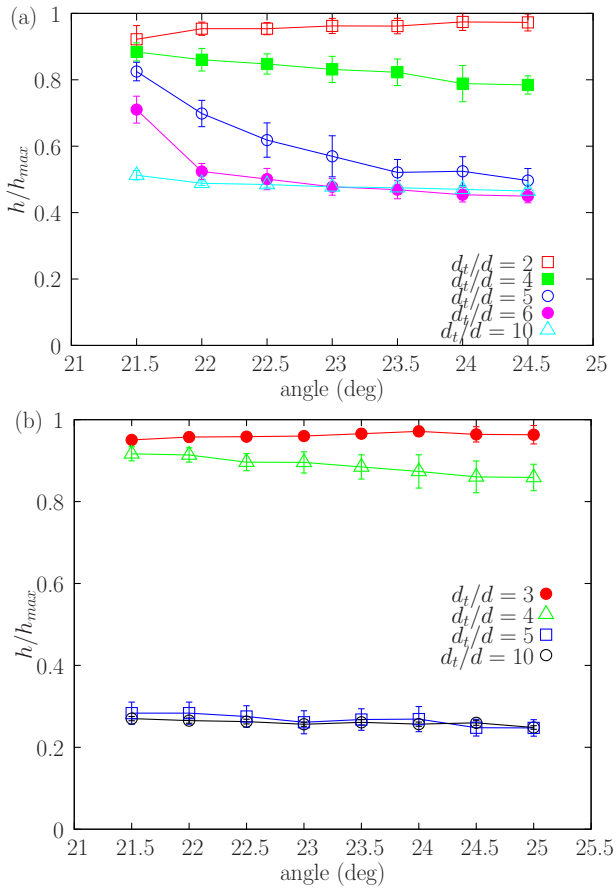

FIG. 22. The relative positions of the tracer flowing down a 3D incline versus slope, for size ratios ranging from $d_t/d = 2$ to 10, for: (a) a thin flow ($h_{max} = 0.112$ m), (b) a thick flow ($h_{max} = 0.223$ m). The error bars show the standard deviations of the vertical position.

In the case of a larger flow, $h_{max} = 0.223$ m, the equilibrium height of the tracer shows almost no dependence with the slope of the incline (Fig. 22(b)). But no size ratios between $d_t/d = 4$ and 5 have been presented here: their behaviour does not present the usual rapid convergence to a final vertical position of equilibrium and needs further investigations. A more extensive study of this phenomenon is ongoing [28].

If time evolution of a tracer position is plotted for different angles (22 to 24°), the tracer sinks more rapidly when the slope is higher (Fig. 23(a)). But if the height is plotted versus the horizontal displacement, all trajectories superimpose (Fig. 23(b)). This shows that a large tracer that reaches its equilibrium height in a reverse segregation phenomenon undergoes a geometrical process. This process is more rapid if the flow velocity increases (higher slope), but the trajectory of the tracer is the same, contrarily to flows with different thicknesses. This result is useful to study multiple tracers flows with a constant thickness.

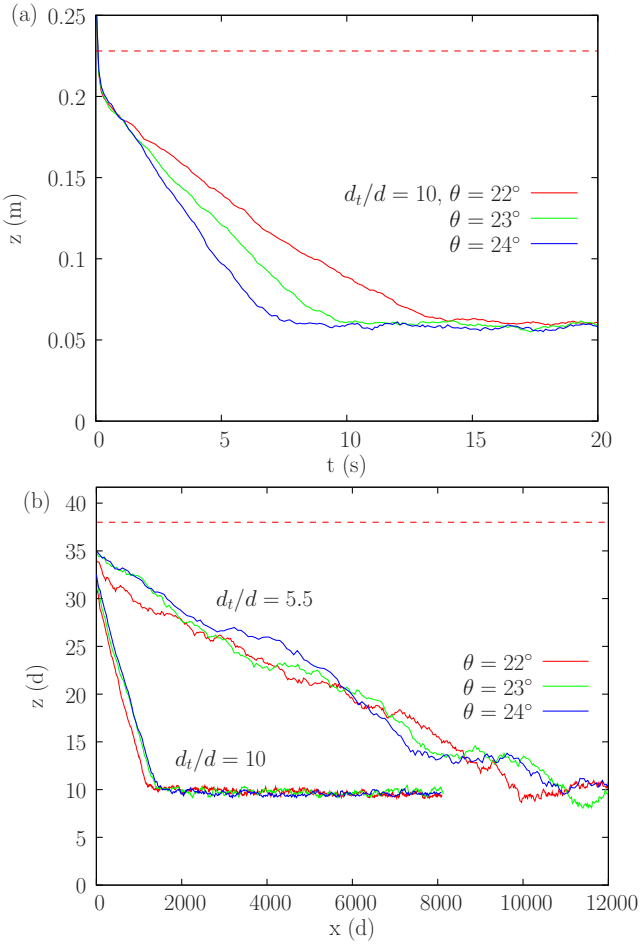

FIG. 23. (a) Time evolution of the tracer height and (b) tracer trajectories (x-z plane) measured in small bead diameters. $d_t/d = 10$, and slope angles are from 22 to 24°. Horizontal dashed line shows the position of the free surface ($h_{max} = 0.223$ m). For comparison, a second, more noisy, trajectories set for a size ratio $d_t/d = 5.5$ is presented.

5. *Multiple tracers flows on incline*

In experiments, several tracers (10% in concentration) were used to increase the measurement statistics [10]. In order to compare with experiments, the effect of the tracer concentration is studied numerically.

The flow mean velocity v have been studied for 3 tracer concentrations (at $d_t/d = 8$) and a flow thickness $h_{max} = 0.223$ m. The mean velocity decreases by a factor 2 while the tracer concentration increases from one tracer ($\simeq 0.8\%$) up to 5%, or to 10%. As pointed out previously (Figs. 11 and 23(b)), if the height of the tracer is studied versus time on flows with non equal velocities, only the stationary height could be compared. For a full comparison of trajectories, vertical versus horizontal displacement should be used.

Figure 24(a) compares the tracer trajectory for flows with a single tracer or with several tracers (10% of the volume). Tracers are initially randomly placed and the

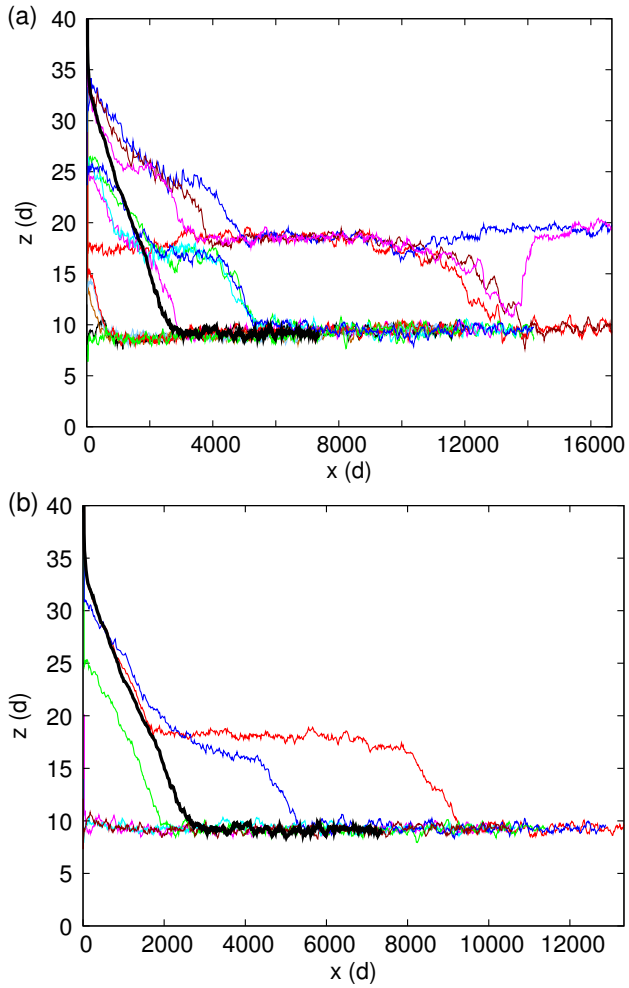

FIG. 24. Tracer trajectories (colored lines) measured in small bead diameter (d) in a flow composed with: (a) 10%, (b) 5% of tracers, compared with the trajectory of a single tracer (thick black line). The thickness of the flow is $h_{max} = 0.223$ m and the size ratio is $d_t/d = 8$.

thickness of the flow is $h_{max} = 0.223$ m $\simeq 37d$. The falling trajectory of a single tracer is more steep compared to the case of multiple tracers. Three, then two, layers of tracers form in the lower part the flow. The height position of the lowest layer in the case of multiple tracers is rapidly identical to the height of one single tracer. Successive down cascading from one layer to another corresponds to an increase of the local fraction of the lowest layers. Very rare up-motion of tracers are observed.

If the concentration of tracers is decreased to 5% (Fig. 24(b)), the falling trajectories slope in the case of a single tracer or in the case of multiple tracers even become comparable. Only one layer of tracers is present, which height is identical to those of a single tracer.

First, the concentration of tracers has no influence on the height of the lowest layer. Consequently, it is possible to compare experimental data and numerical work by the use of lowest numerical trajectories, and experimental lowest tracer positions. The main effect when passing from a single tracer to a fraction of 5, or 10% is the creation of a second, eventually of a third layer above the basal layer of tracers. That corresponds to the fact that the second layer can not disappear by putting its tracers into the first layer, this later being full. The result of the tracer fraction increase is an asymmetric upward spreading of tracers positions, from the lowest layer height.

The same study has been done for other size ratios (see below Fig. 26), around the transition from surface to reverse segregation. For low size ratios ($\leqslant 4$), no major changes are observed for 5% of tracers, except only an increase of the spreading of the positions. For size ratios ($4.2 \leqslant d_t/d \leqslant 4.7$), a higher standard deviation and an up-shift of h are observed, which also makes the curve less steep at the transition. For larger size ratios ($\geqslant 5$), the up-shift is disappearing, and only trajectories are more spread (note that for ratios above 8, all beads fit in the lowest layer giving the same standard deviation than one single particle). Except these little changes, the overall shape of the curve is very close to the behaviour of one single particle. The transition where large tracers plunge into the media, instead of surface-segregating, happens for a similar size ratio. One consequence of the progressive transition between surface and bottom zones is that, at 5%, there is no more an empty central zone for the segregation between the two intermediate segregation layers (Fig. 20). For these fractions, there is a large central zone of intermediate segregation even for this thick (0.223 m) flow, whose organization in three layers looks like those of thin flows.

Secondly, the convergence to the final state of segregation is longer to establish because the falling process is in average, less rapid in the case of 5 or 10% of concentration than the case of one unique tracer. It takes time for tracers to go down from one layer to another. The distance of convergence is so long (around $10000d$) that it is not reached in usual laboratory conditions. Nevertheless, the height of the lowest trajectory is still rapidly defined for thick flows (Fig. 24). In experiments, flows and deposit obtained after the flow stops often present a thickness larger than $37d$. To see how a larger flow thickness affects the previous results, one simulation with a very large thickness $h_{max} = 100d$, $d_t/d = 8$ and a 10% tracer concentration was performed (Fig. 25). Since for a constant tracer fraction, the number of tracer increases with the flow thickness, the number of tracer layers which form in a reverse segregation case, also increases. As several layers of tracers develop (instead of 2 or 3) and as tracers cascade between them, the time and the distance needed for convergence strongly increase (Fig. 25). For experiments, made with d =300-400 μm particles, a distance of convergence of $100000d$ requires an incline of 35 m. Nevertheless, the results obtained are similar than for thinner flows: a reverse segregation for $d_t/d = 8$, the same first layer height of $9d$ than those of thinner flows,

equal to those of a single tracer height (Fig. 24), and the formation of several layers of tracers. However, we may expect shorter convergence times and distances for higher size ratios, since single tracers faster reach their balance level for higher size ratios (Figs. 16 and 17, or 23(b)).

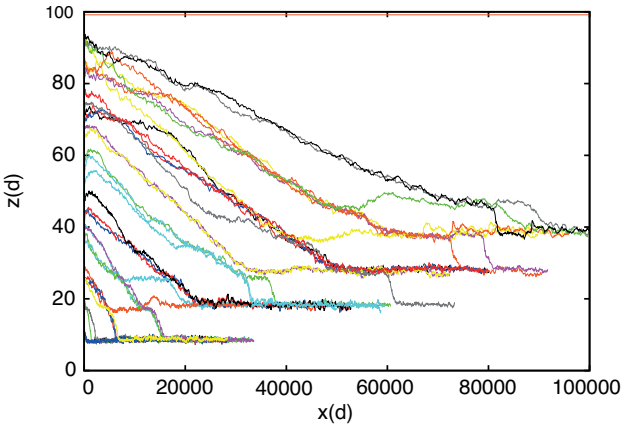

FIG. 25. Trajectories (x-z) of tracers (10%) with a size ratio $d_t/d = 8$, during their sedimentation in a 3D thick flow, h_{max} =100d, measured in small bead diameters.

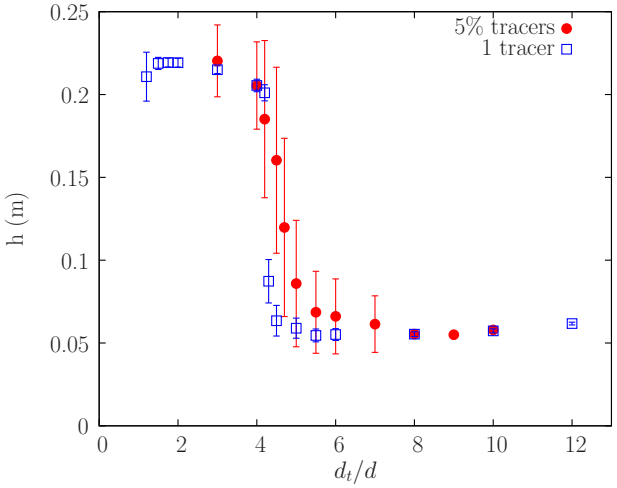

FIG. 26. Equilibrium vertical positions versus size ratio in a 3D incline, for one single tracer (blue □) and for 5% of tracers (red •). The error bars show the standard deviations of the vertical position, but are not representative of the positions distribution of the individual tracers, which are asymmetric: never going upper than the surface or lower than the lowest layer (see Fig. 24). The thickness of the flow is h_{max} = 0.223 m.

6. *Comparison with experiments in channel*

Experiments, made with mixtures of glass beads (10% of tracers), have been done in a 6 cm wide, 1 m long channel, with a slope about 26.5°. Flows have been observed to be 1 to 2 cm thick, with deposits aggraded 2 to 5 cm thick. Results on the established segregation pattern could be separated in three main cases, depending on the size ratio: (1) the small size ratios ($1.75 \leqslant d_t/d \leqslant 3.5$) for which the segregation put all the large tracers at the surface with a small standard deviation, (2) the 4.3 ratio, for which the large tracers are everywhere (surface and inside), and (3) the high ratios ($5.9 \leqslant d_t/d \leqslant 44$) for which the tracers are found inside, with a small layer free of tracers near the surface [10]. A decrease of the average position of the tracers, with a reduction of the standard deviation is observed when increasing the size ratio (for these $d_t/d \geqslant 4.3$).

These three behaviours agree quantitatively with the average positions of tracers found in the simulations (Fig. 26). The up limit of the transition between surface and reverse segregation is experimentally found for 4.3, and this transition happens between 4.2 and 4.3 numerically for one particle, which is a very good agreement. For 5% of tracers, the transition is obtain from 4.2 to 4.7, as the transition is more progressive, still in very good accordance. But experimental standard deviations of tracers are observed to be large, not only for ratio 4.3, but for all high size ratios contrary to simulations, even if they decrease for the higher ratios.

Three experiments have been done in the channel, each with a wall to stop the flow at a given distance (30, 60 and 90 cm) from the start. Tracers are 3 mm, and small beads are 300-400μm (size ratio 8.6). In all cases, tracers are found inside with no major change in the segregation pattern. But the average position of tracers in a slice located at the same distance from the end wall (for example at 10 cm), shows a slight decrease when increasing the length on which the flow propagates. We conclude, that even if the type of segregation is well established, the convergence to a final average position is still developing when the flow stops. All our data, established for a 90 cm traveling distance, do not concern a full stationary state. The process takes longer for 10% to get to their final average height than for one particle. This convergence distance is compatible with those calculated in the simulations, where stationary state is not reached at 2500d (equivalent to 90 cm) for flows of 37d (equivalent to 1.3 cm) (Fig. 24) or for very thick flow of 100d (equivalent to 3.5 cm) (Fig. 25) closer to the deposit thickness. The values of the standard deviation higher than the numerical ones can be explained by the non full converged state and also by the use of 10% of tracers instead of 5%. So, the decrease of the experimental average position and the decrease of the standard deviation for high size ratios could be explained by a better convergence towards the reverse segregated position. This better convergence is compatible with the faster migration of one single particle when increasing the size ratio (comparing Figs. 16 and 17, or Fig. 23(b)). That explains why reverse segregation is experimentally nearly reached for the ratio 44, despite a too short channel.

In the simulations (Figs. 24(a) and 25), for traveling

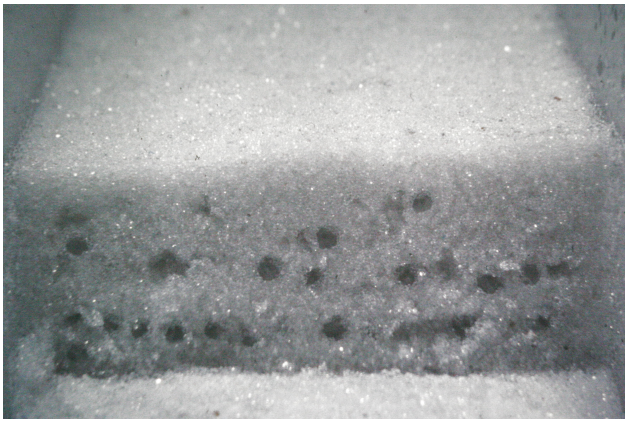

FIG. 27. Slice in the deposit obtained in a 1 m long and 6 cm wide chute flow experiment. The flow is composed of 90% of small beads (300-400μm) and 10% of 3 mm tracers.

lengths corresponding to experiments (90 cm=2500d), tracers above the first layer do not organise in superimposed layers like those obtained at the end of the simulations. For such a flowing distance, only a first bottom layer is already defined, a second one is in formation. The other layers are still emerging and have not reached their final height. Indeed, in experiments, most slices present tracers organised in a bottom layer (Fig. 27), and sometimes in a second one above, not so well defined. Measurements of this bottom layer height have been done between 15 and 30 cm from the front. We choose that to avoid the perturbations due to the collision with the end wall, and the local tracers fraction increase near the front. For size ratios from 4.3 to 15, the bottom layer height is measured from 10 to 11.5d (with a little increase up to 13d for ratio 15, above our simulation parameters range). These values are close to the 9 to 10.2d values found numerically for size ratios from 5 to 12 (Fig. 18).

Even if the stationary stage has not been reached in our experiments, experimental data reproduce well the existence of the bottom layer and its height, the overall transition between surface and reverse segregation, the variation of the associated standard deviations of positions, and the exact ratio (4.3) for which the transition starts. The numerical study also shows that, in experiments, large particles (above the size ratio 5.9) that have settled inside, correspond to non converged states of reverse segregation at different degrees of convergence.

Simulations and experiments agree to show that the size ratio 4.3 induces an intermediate segregation of the tracers, where the spreading of experimental positions (obtained for a non fully converged system) is maximum. The result is a nearly homogeneous mixture of tracers and small beads. This experimental spreading all through the deposit comes of course from the quite large (but smaller) standard deviation shown by the numerical converged result, combined with the average position at an intermediate level. But longer times of convergence, and effects coming from the increase of the tracer fraction might be also implied in the process. For that reason, the range of size ratios around 4.3 needs further investigations.

V. CONCLUSION

In 3D, the segregated position of a large tracer depends mainly on the size ratio between the tracer and the small beads, and on the type of the flow. In the tumbler, a precise study of trajectories has shown that the segregation position is established during the flowing phase and is recorded in the static rotating part. Flow substratum is a loose granular material whose bottom is difficult to define, but trajectories of highest size ratios seem to show tracers at the bottom of the flow. Surface pattern, intermediate segregation with positions going deeper and deeper towards a reverse pattern are observed successively when increasing the size ratio. The transition between surface and reverse segregations is progressive, allowing a large range of tracers size ratios to be in an intermediate segregation pattern.

For all 3D flows down a solid rough incline, two behaviours are very clear: near the surface, which corresponds to tracers on, or just below the surface (surface and intermediate segregation), and near the bottom (intermediate and reverse segregation), which corresponds to tracers floating inside the flow at, or very close to the substratum. Existence of intermediate segregated positions near half-depth, depends on the configuration of the flow and it seems to be not always present. For thick flows, the transition between the two behaviours is sharp, with no tracers stabilised around mid flows. For thin flows, the transition is progressive and a range of tracers stabilised at positions inside the flow, at every intermediate positions. We conclude that, in 3D, the tracer position seems to be determined by the type of substratum (solid, or loose), and by the interaction between surface and bottom when they are close enough, as in thin flows.

On 3D inclines, the three segregation patterns are observed in the case of multiple tracers flows, with a less sharp transition obtained for the same size ratio (around 4.3) for simulations and experiments. But reverse segregation could be long to establish, and a large spreading of the positions stays during a long travel distance. During this travel, the flows could be considered as nearly homogeneous, except near their surface, for size ratios above 5. The choice of a high size ratio could be an opportunity to keep a mixture homogenous for usual industrial transfers. Further studies are needed to set the precise parameters range where this process can be used.

The case of 2D flows have been studied in tumblers and inclines. Compared to the 3D case, they both show a delay in the sinking of the tracer segregated position when increasing its size ratio. Small size ratios behave in relation to surface position as in the 3D case, even if there is a delay. But for large tracers on inclines, the reverse segregation does not exist anymore, even for the largest

size ratios. Tracers stabilise at intermediate positions near mid-flow height, at a position which scales with the flow thickness, contrary to the 3D case. In 2D tumblers, the position evolution is also delayed and shifted with a radial intermediate segregation of the largest tracers. However, this radial position does correspond to reverse levels comparable to those of the 3D case, but still with a delay. The discrepancy between 2D and 3D, probably due to the compacity difference between 2D and 3D, does not affect all the processes implied in the segregation in the same manner. The highest care should be taken before extrapolating results of studies between 2D and 3D cases.

ACKNOWLEDGMENTS

The authors thank J. Favier for the careful rereading of this notes. This work was granted access to the HPC resources of Aix-Marseille Université financed by the project Equip@Meso (ANR-10-EQPX-29-01) of the program " Investissements d'Avenir " supervised by the Agence Nationale de la Recherche.

[1] J. C. Williams, Powder Technol. **15**, 245 (1976).
[2] J. Duran, J. Rajchenbach, and E. Clément, Phys. Rev. Lett. **70**, 2431 (1993).
[3] J. B. Knight, H. M. Jaeger, and S. R. Nagel, Phys. Rev. Lett. **70**, 3728 (1993).
[4] F. Cantelaube and D. Bideau, Europhys. Lett., **30** (3), 133 (1995).
[5] K. Hutter, B. Svendsen, and D. Rickenmann, Contin. Mech. Thermodyn. **8** (1) 1 (1996).
[6] J. M. Ottino and D. V. Khakhar, Annu. Rev. Fluid Mech., **32** (1) 55 (2000).
[7] J. M. N. T. Gray, M. Shearer, and A. R. Thornton, Proc. R. Soc. A **462**, 947 (2006).
[8] F. Guillard, Y. Forterre, and O. Pouliquen, Phys. Fluids **26**, 043301 (2014).
[9] C. P. Schlick, Y. Fan, P. B. Umbanhowar, J. M. Ottino and R. M. Lueptow, J. Fluid Mech. **765**, 632 (2015).
[10] N. Thomas, Phys. Rev. E **62**, 961 (2000).
[11] G. Félix and N. Thomas, Phys. Rev. E **70**, 051307 (2004).
[12] T. Shinbrot and F. J. Muzzio, Phys. Rev. Lett **81** (20) 4365 (1998).
[13] A. P. J. Breu, H.-M. Ensner, C. A. Kruelle, and I. Rehberg, Phys. Rev. Lett. **90** (1) 014302 (2003).
[14] J. Ellenberger, C. O. Vandu, and R. Krishna, Powder Technol. **164** (3), 168-173 (2006).
[15] D. Hong, P. V. Quinn and S. Luding, Phys. Rev. Lett. **86** (15) (2001).
[16] J. B. Knight, H. M. Jeager and S. R. Nagel, Phys. Rev. E **70** (24) (1993).
[17] J. Schäfer, S. Dippel and D. E. Wolf, J. Phys 1 (France) **6**, 5 (1996).
[18] P. A. Cundall and O. D. L. Starck, Géotechnique **29**, 47 (1979).
[19] T. G. Drake and R. L. Shreve, J. Rheol. **30**, 981 (1986).
[20] S. F. Foerster, M. Y. Louge, H. Chang, and K. Allia, Phys. Fluids **6**, 1108 (1994).
[21] Z. Zaman, U. D'Ortona, P. B. Umbanhowar, J. M. Ottino and R. M. Lueptow, Phys. Rev. E **88**, 012208 (2013).
[22] N. Taberlet, M. Newey, P. Richard, and W. Losert, J. Stat. Mech. P07013 (2006).
[23] P. Chen, J. M. Ottino, and R. M. Lueptow, New J. Phys. **13**, 055021 (2011).
[24] G. H. Ristow, Pattern Formation in Granular Materials (Springer-Verlag, Berlin, 2000).
[25] C. S. Campbell, J. Fluid Mech. **465**, 261 (2002).
[26] L. E. Silbert, G. S. Grest, R. Brewster, and A. J. Levine, Phys. Rev. Lett. **99**, 068002 (2007).
[27] G. Félix and N. Thomas, Earth Planet. Sci. Lett. **221**, 197-213 (2004).
[28] N. Thomas and U. D'Ortona, in prep.